



## 29<sup>th</sup> International Conference on Lightning Protection

23<sup>rd</sup> – 26<sup>th</sup> June 2008 – Uppsala, Sweden



### PARAMETERS OF LIGHTNING CURRENT GIVEN IN IEC 62305 – BACKGROUND, EXPERIENCE AND OUTLOOK

F. Heidler

University of the Federal Armed Forces Munich, Germany  
Wolfgang.Zischank@unibw.de

W. Zischank

University of the Federal Armed Forces Munich, Germany  
Fridolin.Heidler@unibw.de

Z. Flisowski

University of Technology Warsaw, Poland  
Zdobyslaw.Flisowski@ien.pw.edu.pl

Ch. Bouquegneau

Faculté Polytechnique de Mons, Belgium  
Christian.Bouquegneau@fpms.ac.be

C. Mazzetti

University “La Sapienza” Rome, Italy  
Carlo.Mazzetti@uniroma1.it

University of the Federal Armed Forces Munich, EIT 7, Werner-Heisenberg-Weg 35, 85577 Neubiberg

**Abstract - The Technical Committee TC 81 “Lightning Protection” of the International Electrotechnical Commission IEC was established in Stockholm in June 1980 with the scope to prepare international standards and guides for lightning protection for structures and buildings, as well for persons, installations, services and contents. Meanwhile, the results of TC 81 are published in the international standard series IEC 62305.**

TC 81 decided as one of the first steps to define the lightning threat as a common basis to any protection measures. The lightning threat is mainly derived from the measurements of *Berger* performed at two 70 m towers on the Mountain San Salvatore in Switzerland. Up to now, the results published in CIGRE Electra in 1975 [16] and 1980 [33] represent the most complete data base of lightning currents and their relevant parameters.

The paper reviews the various types of lightning ground flashes, the current components relevant for protection and the current parameters obtained from measurements. On the basis of these measurements, some background information is given how TC 81 selected the parameters published in IEC 62305-1. Finally, methods to simulate lightning currents in laboratory are presented which allow the verification of lightning protection measures or components.

#### 1 INTRODUCTION

Up to the beginning of the 20th century lightning protection measures were mostly based on empirical knowledge. The scientific era of lightning research started not until technologies like photography and oscilloscopes became available.

Once it had been established early in the 20th century that the lightning current is almost invariably unidirectional, Ampere’s law could be used to measure the current peak value with small magnetic links. Small bundles of parallel steel wires were located in glass tubes [1]. The magnetic links were installed close to the down conductors, where in case of a lightning strike they became magnetized. The peak value of the lightning current and the polarity could then be derived from the residual magnetism retained by the steel wires. Because the magnetic links were relatively cheap, ten thousands of them were installed at high-voltage power lines in Germany [2, 3]. Similar experiments were carried out at high-voltage power lines and other high objects in Russia [5] and at high chimneys in Poland [6]. In Czechoslovakia more than 1000 lightning currents were measured from 1958 to 1985 at buildings with heights ranging from 25 m up to 140 m [4].

Probably *McEachron* was the first who recorded the current waveform with oscilloscopes, when he measured the lightning currents at the Empire State Building in New York, USA during the thirties of the last century [7]. The use of storage oscilloscopes allowed resolving the whole current waveform including the fast rising current front and the slow decay. With this method, *Berger* measured the lightning currents at two 70 m high towers on the mountain San Salvatore, Switzerland. During a period of about 10 years *Garbagnati* and *LoPiparo* recorded lightning currents at two 40 m high telecommunication towers located at Foligno and Monte Orsa in Italy [8]. In South Africa the lightning currents were measured for more than 15 years at a 60 m high mast [9]. Because the probability of lightning strikes increases with the structure height, in Russia even tethered balloons were used to erect a 1000 m high steel wire [11].

Most of the lightning strikes to tall towers are upward discharges developing from the top of the structure. At very high towers, like the 540 m high Ostankino tower in Moscow, Russia, however, it was found that lightning may also terminate at the lower parts of the tower [12, 13]. More recently upward lightning was measured at the Peissenberg tower in Germany [22], the Gaisberg tower in Austria [23], the CN-tower in Canada [24] and the San Chrischona tower in Switzerland [25]. The upward lightning typically occur in winter when the thundercloud base is lower and closer to the tower top. From the measurements in Japan at several high objects it is known that the lightning during winter thunderstorm may be very severe transferring high charges to ground [14, 15].

Because even at high towers the number of lightning strikes is restricted to a few up to some ten events per year [26], rockets are used to artificially trigger the lightning discharges. The rocket quickly brings up a trailing metal wire in a strong electric field which acts similar to a high tower where upward discharges are initiated. *Newman* was the first who did such experiments when he started rockets from a boat located at the coast of Florida in 1962 [27]. Meanwhile triggered lightning experiments have been performed by several research group, e.g in Japan [28], China [29], France [30] and the USA [31, 35, 36]. The results reveal that the rocket triggered upward lightning has current components similar to the current component of normal upward lightning.

The most important data originate from the experiments of *Berger* who measured the lightning currents from 1943 to 1971 at two telecommunication towers on the mountain San Salvatore, Switzerland. The top of this mountain is 915 m above sea level and 640 m above the Lake of Lugano. Both towers have a height of 70 m including the Franklin rod installed at the top. All in all, the currents of more than one thousand upward and more than 200 downward lightning discharges could be successfully recorded during this extensive measuring period [16-21]. Up to now, these results published in [16, 33] are the basis for the lightning protection standard series IEC 62305 edited by the Technical committee TC 81 of IEC.

## 2 TYPES OF LIGHTNING TO GROUND

In general, flashes that lower negative charge to ground are termed negative lightning, while those that transfer positive charge to ground are referred to as positive lightning. Due to their initiating leader process, they are further classified into downward lightning and upward lightning.

### A. Downward lightning

Small buildings up to about 100 m are almost exclusively struck by downward lightning. The lightning discharge starts with a leader inside the thundercloud propagating down towards ground. The negative downward lightning has a negative downward leader, while the positive downward lightning has a positive downward leader, as illustrated in Fig. 1a, Fig. 1b.

When the downward propagating leader approaches ground the electric field at grounded objects increases due to the charge contained in the downward leader channel. As soon as the electric field exceeds a certain level, connecting leaders start from the grounded objects making the final connection between the objects at ground and the downward leader. This is the beginning of the return stroke phase, where the return stroke current flows through the struck object.

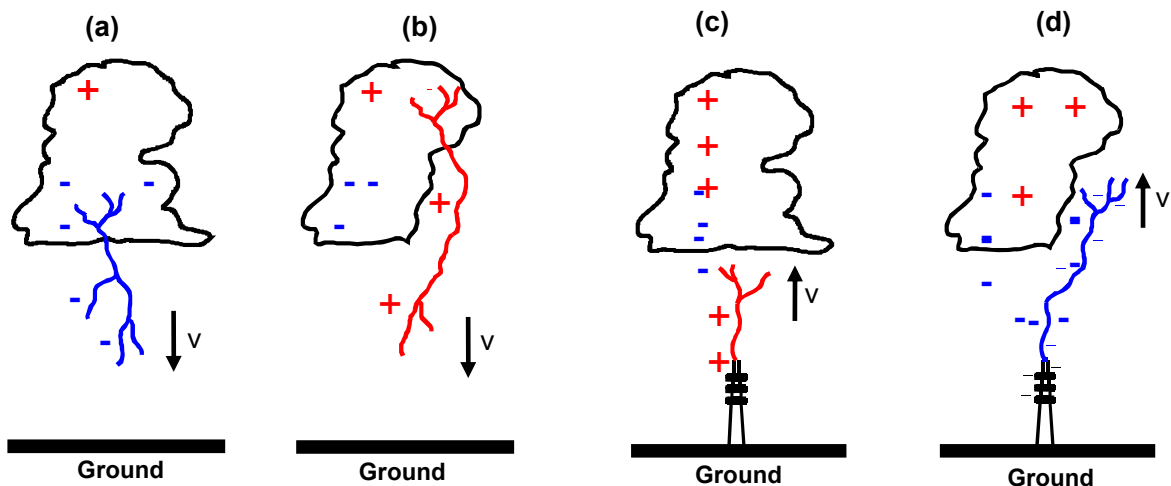


Fig. 1 - Types of lightning flashes to ground comprising (a) negative downward lightning, (b) positive downward lightning, (c) negative upward lightning, and (d) positive upward lightning

Fig. 2 shows two examples for the current of the first positive and the first negative return stroke. The peak values are typically in the range of several 10 kA. Especially positive first stroke may exhibit high peak currents, exceeding the value of 100 kA. The impulse currents of the return strokes have a fast rising front with a front time ranging from several 100 ns up to more than 10  $\mu\text{s}$  and a slowly dropping decay. The currents of the negative first return stroke typically cease after some 100 $\mu\text{s}$  (Fig. 2 b), while currents of the positive strokes may last significantly longer up to more than 2 ms (Fig. 2 b). Due to the longer duration, the positive return stroke currents transfer more charge to ground compared to the negative first return stroke current.

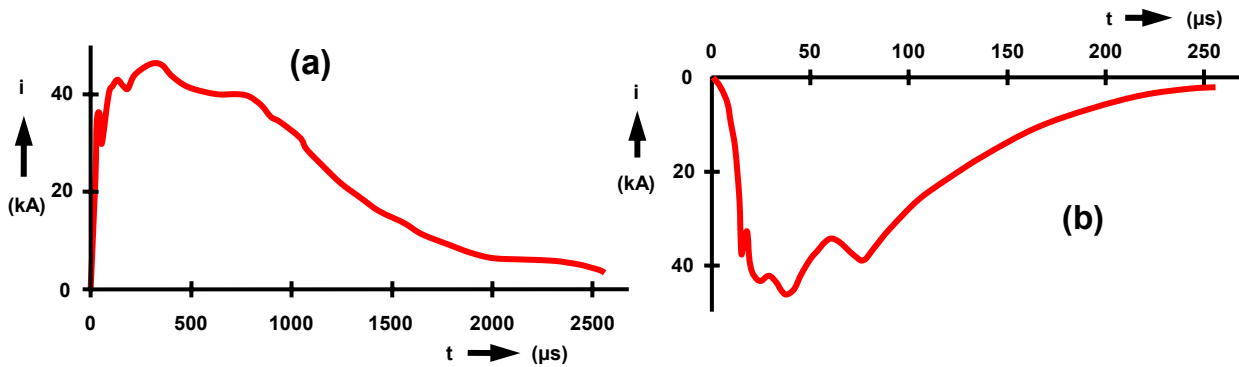


Fig. 2 – Return stroke currents of first strokes of (a) positive and (b) negative downward lightning according to Berger

The first return stroke may be followed by several subsequent return strokes following the same lightning channel. About 3/4 of the negative downward flashes contain more than one return stroke. On the average such multiple stroke flashes consist of a first return stroke and about 3 subsequent return strokes. On contrast, the only few positive downward flashes contain multiple strokes. The positive downward lightning mostly has a first return stroke without any subsequent stroke.

Fig. 3 shows the current of a multiple negative downward flash consisting of 11 return strokes and one continuing current. The continuing currents always follow immediately after a return stroke current, in Fig. 3 after the 8<sup>th</sup> return stroke. The peak currents of the subsequent return stroke are in the range of 10 kA and thus much smaller than the peak currents of the first strokes. On the other hand, the subsequent return strokes have short rise times and therefore higher di/dt-values compared to the first return strokes. The continuing currents differ from the return stroke currents significantly having much lower current amplitudes in the range of some 100 A, but much longer duration in the range of some 100 ms.

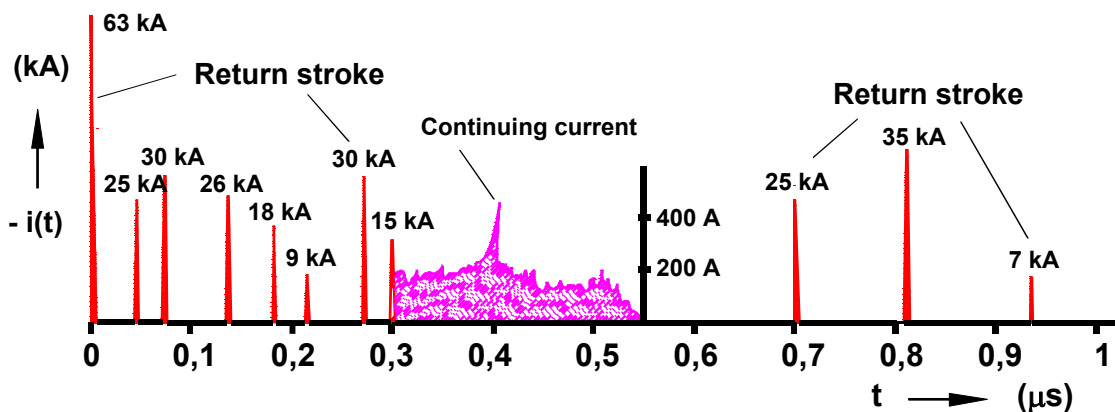


Fig. 3 – Current of a multiple stroke negative downward lightning with 11 return strokes and one continuing current

### B. Upward lightning

The electric field at the top of a structure increases with the object height. At a tall building the electric field may be enhanced to such an extent that an upward leader starts from the top of it. To exceed the critical electric field strength, the object must have a height of about 100 m at minimum. The upward propagating leader is associated with an initial continuous current flow through the object. Fig. 1c and Fig. 1d show, that the upward leader is positive in case of negative upward lightning and negative in case of positive upward lightning. Fig. 4 shows the current of a negative upward flash measured at the Peissenberg tower, Germany. Impulse currents are superimposed to the initial continuous current. These so-called  $\alpha$ -components are short duration currents with amplitudes up to several kA. After the cessation of the initial continuous current  $\beta$ -components may follow, which are similar to the currents of the subsequent return strokes. Furthermore, a small continuing current may occur immediately after a  $\beta$ -component as shown in Fig. 4.

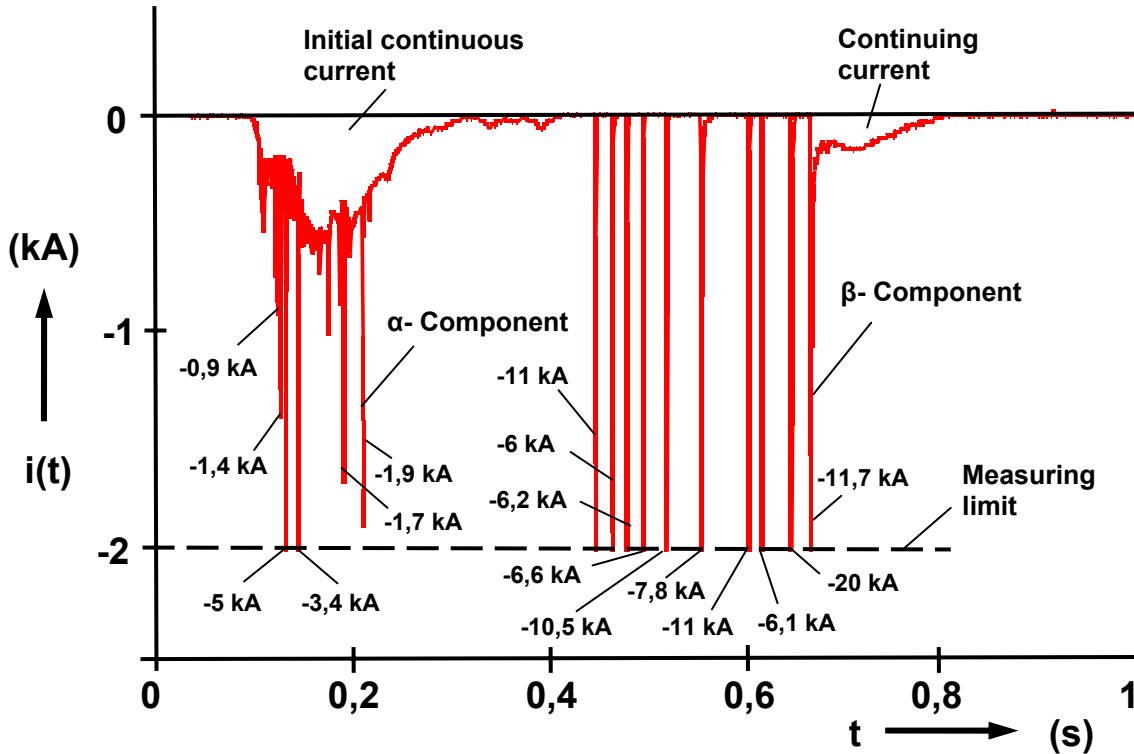


Fig. 4 – Current of a negative upward lightning measured at the Peissenberg tower, Germany.

### 3 COMPARISON OF THE MEASUREMENTS OF THE CURRENT PEAK

Most of the data available for natural lightning currents are related to the current peak value. The average values of the current peak are listed in Table 1 and Table 2 for the first and subsequent return stroke of downward lightning. Because the triggered lightning and the  $\beta$ -components of the upward lightning are similar to the subsequent return stroke, they are also included in Table 2.

From Table 1 it can be seen that the average values of the current peak are in the range of about 30 kA for both, positive and negative first return strokes. At the Peissenberg tower only one negative downward flash was recorded up to now, so that an average value can not be given. For the 5 positive first return strokes measured at Foligno and Monte Orsa only a range of the currents exceeding about 30 kA is reported in [8] and a clear separation between upward and downward flashes could not be made. Table 2 shows that the average values of the current peaks of the negative subsequent strokes vary from 8 kA to 18 kA, the mean value being about 12 kA.

The values obtained from the experiments of *Berger* at the Monte San Salvatore are about in the middle of the range reported from the various the measurement stations. Because of that, the ‘International Council on Large Electric Systems’ (CIGRE) accepted the Monte San Salvatore data as references for the lightning currents. The statistics of the data are published in CIGRE Electra [16, 33]. Registration results of lightning location systems don’t change, as till now, the validity of CIGRE lightning data.

Table 1: Average values of the current peak of first return stroke

Location	Positive first		Negative first		Remarks
	Number	50 %-value kA	Number	50 %-value kA	
Monte San Salvatore, Switzerland [16]	26	35	101	30	Tower height 70 m
Masts of overhead power lines, Germany [3]	28	23 <sup>1)</sup>	224	29 <sup>1)</sup>	Magnetic links
Objects of 25 - 140 m height, Czechoslovakia [4]	224	30	1015	28 <sup>1)</sup>	Magnetic links
Peissenberg tower, Germany [34]	-	-	1	(54)	Tower height 160 m
Morro do Cachimbo Station, Brazil [10]	-	-	31	45,3	60 m high mast
South Africa [9]			29	43	60 m mast
Foligno and Monte Orsa, Italy [8]	5	(30 - 160)	42	33	40 m high towers

<sup>1)</sup> arithmetic mean value

Table 2: Average values of the current peak of the negative subsequent return stroke

Location	Number	50 %- value kA	Remarks
Monte San Salvatore, Switzerland [16]	135	12	Tower height 70 m
Morro do Cachimbo Station, Brazil [10]	59	16,3	60 m high mast
South Africa [9]	-	~ 8	60 m mast
Camp Blanding, Florida [35]	64	14,5	Triggered lightning
Peissenberg tower, Germany [22]	35	8,5	Tower height 160 m, $\beta$ -components
Saint-Privat d'Allier, France [30]	54	9,8	Triggered lightning
Florida [30]	305	12,1	Triggered lightning
Foligno and Monte Orsa, Italy [8]	33	18	40 m high towers
Alabama [36]	45	12	Triggered lightning

#### 4 LIGHTNING CURRENTS PARAMETERS RELATED TO MECHANICAL, THERMAL AND INDUCTION EFFECTS

##### C. Relevant current parameters for the lightning protection

The current is the primary source for all thermal and mechanical damages caused by lightning. Besides that, the rate-of-rise of the lightning currents may induce overvoltages in electric and electronic systems or devices. The lightning threat is associated with the following current parameters:

- Current peak  $i_{\max}$
- Charge  $Q = \int i \cdot dt$
- Specific energy  $W / R = \int i^2 \cdot dt$
- Maximum current derivative  $\left( \frac{di}{dt} \right)_{\max}$

The peak current is important for the design of the earth termination system. When the lightning current enters the earth, the current flowing through the earthing resistance produces a voltage drop. The peak current determines the maximum value of this voltage drop. This voltage drop may lead to side flashes when conductive services lines enter a building unbonded.

The charge Q is responsible for the melting effects at the attachment points of the lightning channel. The energy input at the arc root is given by the anode/cathode voltage drop multiplied by the charge Q.

The specific energy W/R is responsible for mechanical forces and for the heating effects, when the lightning current flows through metallic conductors.

Electronic devices are normally connected to different electrical services as the mains supply and the data link. Depending on the line routing inside a structure, large loops may be formed by these lines. The maximum current steepness determines the maximum of the magnetically induced voltages into open loops.

#### D. Current components

The measurements revealed that the current parameters of the upward lightning do not exceed the current parameters of the downward lightning. Because no additional threat has to be taken into account for the upward lightning, the current components codified in the standard IEC 62305-1 [32] are exclusively based on the currents of the downward lightning. In order to represent the threat of the lightning currents, the following basic current components are fixed in the standard IEC 62305-1 [32]:

- First short stroke current
- Subsequent short stroke current
- Long stroke current

The first short stroke current takes into account the threat of the first return strokes of downward lightning. The threat of the first return strokes mainly originates from the positive lightning having higher current peaks  $i_{max}$ , higher impulse charge  $Q_i$  and higher specific energy  $W/R$  compared to the negative lightning. According to the measurements of *Berger*, a relatively strong correlation exists between these three current parameters. In Table 3 the correlation coefficients between parameters of positive return strokes are reproduced from [16]. In order to reproduce the thermal and mechanical threats of first return strokes, the current peak, the impulse charge and the specific energy have to be simulated simultaneously within one current impulse.

*Berger* also showed that there is only a weak correlation between the rise time or the maximum current steepness and the other parameters. Therefore, the threat presented by the current steepness during the fast rising front can be taken into account separately by a subsequent short stroke current. Fig. 5 shows the waveform definitions for the short stroke currents. The short stroke current has a fast rising front characterized by the front time  $T_1$  and a slow decay characterized by the decay time to half-value  $T_2$ .

The long stroke current, finally, takes into account the charge transfer of the continuing currents. Fig. 6 shows the definitions for the long stroke current, where the charge and the duration of the current are fixed.

Table 3: Correlation coefficients between parameters of positive return strokes

	Peak current	Front time	Current steepness	Impulse charge	Specific energy
Peak current	1				
Front time	0,07	1			
Current steepness	0,49	- 0,68	1		
Impulse charge	<b>0,77</b>	0,27	0,23	1	
Specific energy	<b>0,84</b>	0,22	0,39	<b>0,82</b>	1

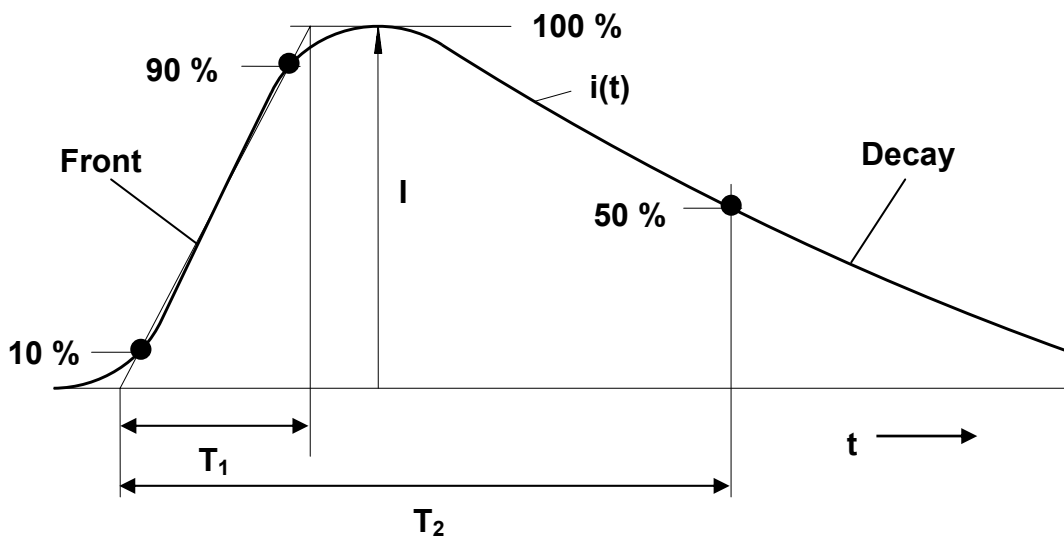


Fig. 5 – Definition of the short stroke current where  $T_1$  is the front time and  $T_2$  is the decay time

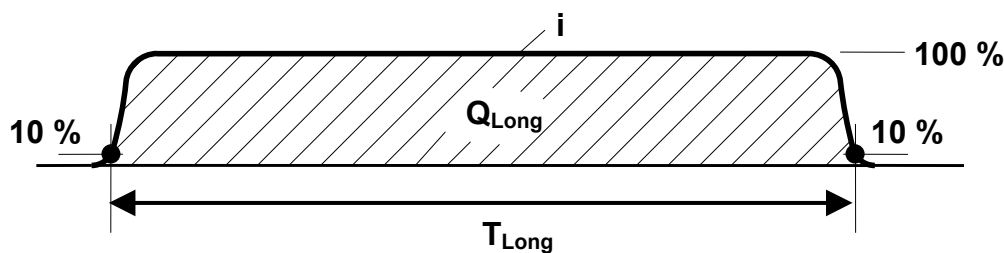


Fig. 6 – Definition of the long stroke current

**E. Definition of the lightning protection level LPL**

In IEC 62305-1 four lightning protection levels LPL have been introduced to take into account the different safety requirements of various buildings. For instance, a dwelling house requires a lower safety level than a plant handling explosive materials.

For a reliable protection against the thermal and mechanical effects of lightning as well as induced over-voltages the current parameters at the upper end of the statistical lightning current distributions have to be taken into account. It was the intention of TC 81 that the parameters fixed for LPL I shall not be exceeded in naturally occurring lightning with a probability of about 99 %. For the LPL II the parameters of LPL I are reduced to 75 % and for LPL III and LPL IV to 50 % of LPL I. The reduction follows a linear relationship for peak current, impulse charge and current steepness, but a quadratic one for the specific energy.

**F. Positive lightning**

As stated above, it was the intention of TC 81 to cover about 99 % of all lightning for protection level LPL I. As a consequence positive lightning can not be omitted. Positive lightning may vary seasonally and in different regions of the world. However, instrumented tower measurements as well as lightning locating systems [e.g. 37, 38] show that it accounts for about 10 % of the global cloud-to-ground lightning activity. Positive lightning even can be the dominant type of cloud-to-ground lightning during the winter season or during the dissipating stage of a thunderstorm.

The positive lightning current waveforms observed by Berger can be divided into two categories [39]: The first category involves microsecond-scale waveforms similar to those for negative lightning, and the second one millisecond-scale waveforms with long rise times up to hundreds of microseconds. Examples of the two types of current waveform are shown in Fig. 7 and Fig. 8.

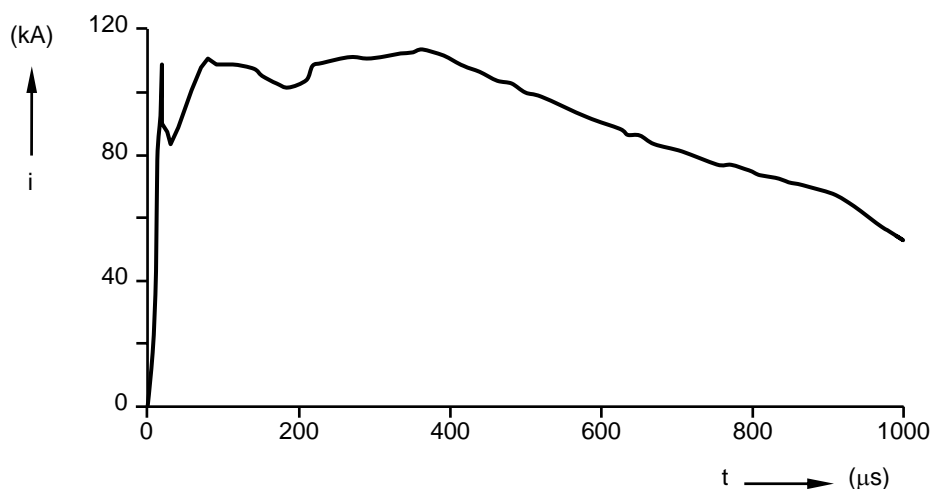


Fig. 7 - Microsecond-scale waveform of positive lightning adapted from Berger

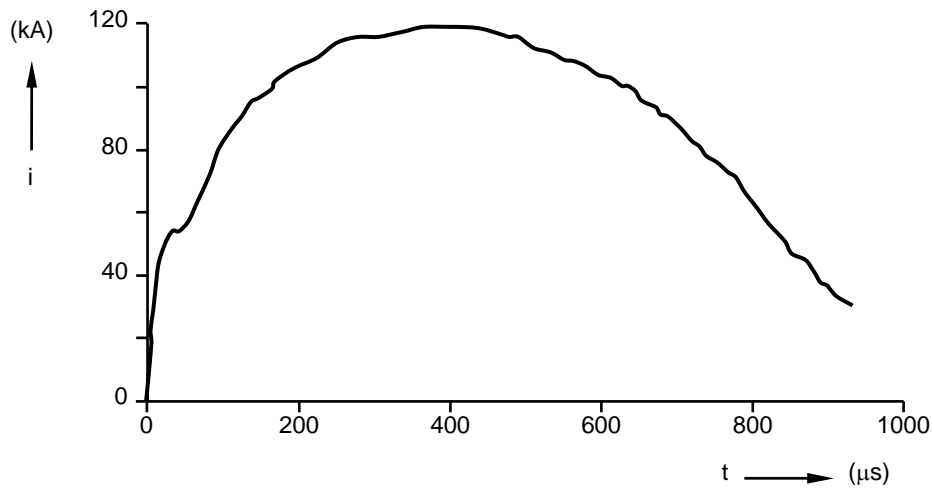


Fig. 8 - Millisecond-scale waveform of positive lightning adapted from *Berger*

*Rakov* [39] concludes that the “microsecond-scale waveforms are probably formed in a manner similar to that in downward negative lightning, while millisecond-scale waveforms are likely to be a result of the M-component mode of charge transfer to ground”. In the absence of tall structures, most positive lightning is likely to be initiated by a positively charged downward leader. The highest directly measured currents were found for positive lightning including a charge transfer of a few 100 C. An example of a positive  $\sim 320$  kA current measured by *Goto* [14] is reproduced in Fig. 9.

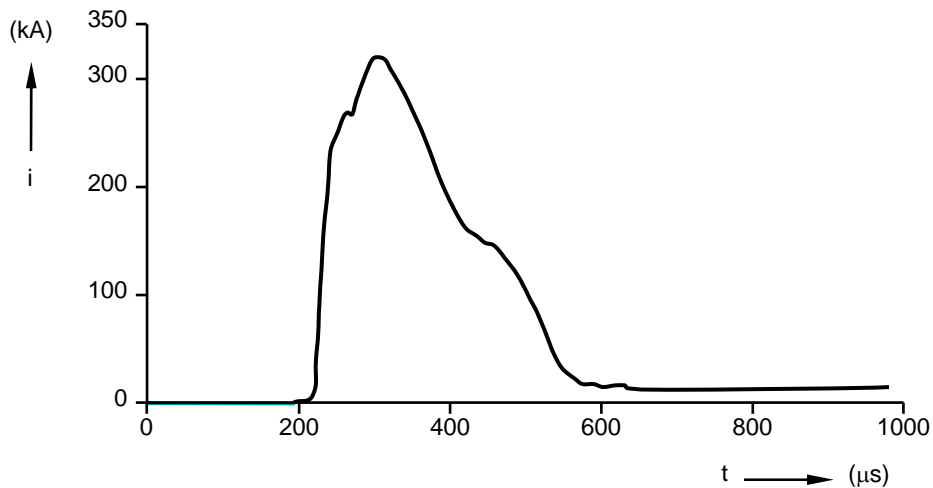


Fig. 9 - 300 kA positive lightning current adapted from *Goto*

### G. Fixing of the current parameters

The standard IEC 62305-1 originally was based on the lightning parameters obtained from the experiments of *Berger*. As mentioned above, the statistics of the measured current parameters are published in two landmark papers in *CIGRE Electra* [16, 33]. In IEC 62305-1 the positive and negative first strokes are considered in common weighted statistics, because most damages caused by lightning do not significantly depend on the direction of the current flow. According to their occurrence, the negative first strokes contribute about 90 % and the positive first stroke about 10 % to the common statistics of the first short stroke current parameters.



The fixing of the current parameters is explained for the lightning protection level LPL I where only 1 % of the naturally occurring lightning currents shall exceed the standardized values (see Table 4). Positive lightning dominates the upper end of the statistics. Since only 1/10 of all lightning is positive, it is sufficient to cover about 10 % of positive lightning in order to achieve the intended 99 % protection. From Fig. 10 it can be seen that a current peak value of 200 kA meets the aim of TC 81. Applying the same rationale for the impulse charge (Fig. 11) and the specific energy (Fig. 12) leads to values of  $Q_i = 100 \text{ C}$  and  $W/R = 10 \cdot 10^6 \text{ J}/\Omega$  for LPL I. Similarly, the charge transfer of the long stroke current  $Q_l$  follows by subtracting the impulse charge  $Q_i$  from the total flash charge  $Q_{\text{total}}$  of positive lightning, i.e.  $Q_l = Q_{\text{total}} - Q_i = 300 \text{ C} - 100 \text{ C} = 200 \text{ C}$  for LPL I.

The fixed values of the peak current, the charge and the specific energy predefine the waveform of the first short stroke current during its decay. For an exponentially decaying current waveform of

$$i = i_{\text{max}} \cdot \exp\left(-\frac{t}{\tau}\right) \quad (1)$$

the parameters  $Q$  and  $W/R$  can be determined by

$$Q = i_{\text{max}} \cdot \tau \quad (2)$$

and

$$W/R = i_{\text{max}}^2 \cdot \frac{\tau}{2}. \quad (3)$$

The time constant  $\tau$  is related to the decay time-to-half value  $T_2$  by

$$\tau = T_2 / \ln(2). \quad (4)$$

With the parameters  $i_{\text{max}} = 200 \text{ kA}$ ,  $Q = 100 \text{ C}$  and  $W/R = 10 \cdot 10^6$  a time constant of  $\tau = 500 \mu\text{s}$  and thus a decay time-to-half value of  $T_2 = 350 \mu\text{s}$  follows from the above equations. Because the correlation between the parameters for the rise time portion and the other current parameters is weak (see Table 3), there is no special requirement to the rise time of the first short stroke current. Therefore, the rise time was chosen to  $T_1 = 10 \mu\text{s}$ , which is a typical value for the cloud-to-ground positive return strokes.

From Fig. 10 it can be seen that the current peak of negative subsequent strokes associated with the 1 % -probability is about 40 kA. In order to give a rounded figure, TC 81 fixed a value of 50 kA. This also takes care of the fact that a flash may contain several subsequent strokes: Because a multiple negative downward lightning has an average of about 3 subsequent return strokes, a building is struck 3 times by a subsequent return stroke during one flash. Therefore, the probability to be taken into account becomes one third of the intended 1 %, i.e. 0,3 %.

With respect to the current steepness, positive lightning can be omitted because the current normally does not have a high rate-of-rise. The highest current steepness is found in negative subsequent stroke as can be seen from Fig. 13. The average current steepness between the 30 % and the 90 % current level of negative subsequent strokes is about 200 kA/ $\mu\text{s}$ . This value is taken in IEC 62305-1 as average current steepness. Thus, for the subsequent short stroke current a rise time  $T_1 = 50 \text{ kA} / 200 \text{ kA}/\mu\text{s} = 0.25 \mu\text{s}$  follows. Due to the limited time resolution of about 500 ns of *Berger's* recording system, it is likely that the  $di/dt$  values are biased toward lower values. Extrapolating the *maximum* current derivative to a 1 % level would result in  $(di/dt)_{\text{max}} = 280 \text{ kA}/\mu\text{s}$ . As the subsequent short stroke is mainly intended to simulate the fast rising portion of the current, the current decay is of minor interest and in IEC 62305-1 a typical value of  $T_2 = 100 \mu\text{s}$  has been chosen.

The lightning parameters of the lightning protection levels LPL II and LPL II/IV are derived from LPL I as explained earlier by reducing the LPL I parameters to 75 % for LPL II and to 50 % for LPL III/IV. The waveforms remain unchanged. The current peak value, the charge and the maximum current steepness are to be reduced linearly. Because the specific energy is proportional to  $i^2$ ,  $W/R$  is reduced by the factor  $(4/3)^2$  for LPL II and by the factor 4 for LPL III/IV. Table 4 summarizes the lightning parameters for the different LPL.

Table 4: Maximum values of the current parameters due to the different lightning protection levels LPL

First short stroke current			LPL		
Current parameter	Symbol	Unit	I	II	III/ IV
Maximum of the first short stroke current	$i_{max}$	kA	200	150	100
Charge of the first short stroke current	$Q_{short}$	C	100	75	50
Specific energy of the first short stroke current	W/R	MJ/ $\Omega$	10	5,6	2,5
Wave form	$T_1/ T_2$	$\mu s/\mu s$	10/350		
Subsequent short stroke current			LPL		
Current parameter	Symbol	Unit	I	II	III/IV
Maximum of the subsequent short stroke current	$i_{max}$	kA	50	37,5	25
Average front steepness of the subsequent short stroke current	$di/dt$	kA/ $\mu s$	200	150	100
Wave form	$T_1/ T_2$	$\mu s/\mu s$	0,25/100		
Long stroke current			LPL		
Current parameter	Symbol	Unit	I	II	III/IV
Charge of the long stroke current	$Q_{long}$	C	200	150	100
Duration of the long stroke current	$T_{long}$	s	0,5		
Lightning flash			LPL		
Current parameter	Symbol	Unit	I	II	III/IV
Charge of the total lightning flash	$Q_{flash}$	C	300	225	150

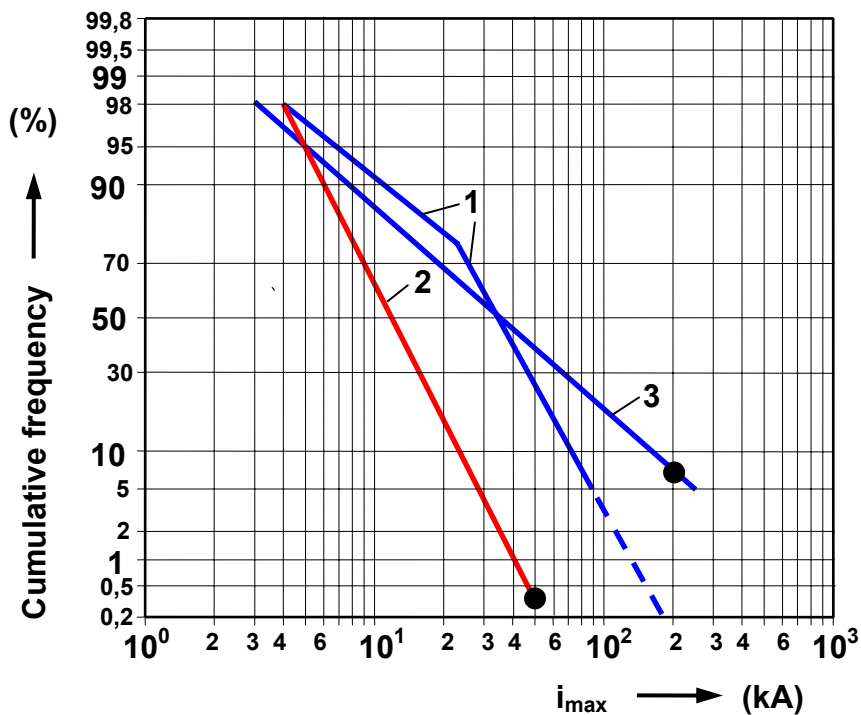


Fig. 10 - Cumulative frequency of the current peak  $i_{max}$  according to CIGRE

1: Negative first stroke

2: Negative subsequent stroke

3: Positive stroke

● Fixed value in IEC 62305-1 for LPL 1

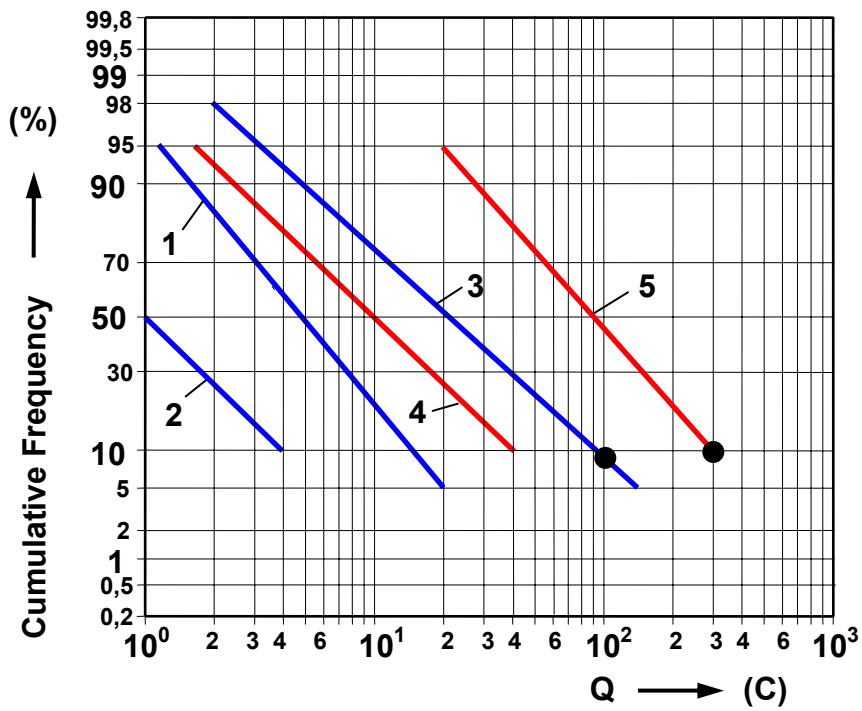


Fig. 11 – Cumulative frequency of the charge Q according to CIGRE  
 1: Negative first stroke  
 2: Negative subsequent stroke  
 3: Positive stroke  
 4: Total charge of the negative stroke  
 5: Total charge of the positive stroke  
 • Fixed value in IEC 62305-1 for LPL 1

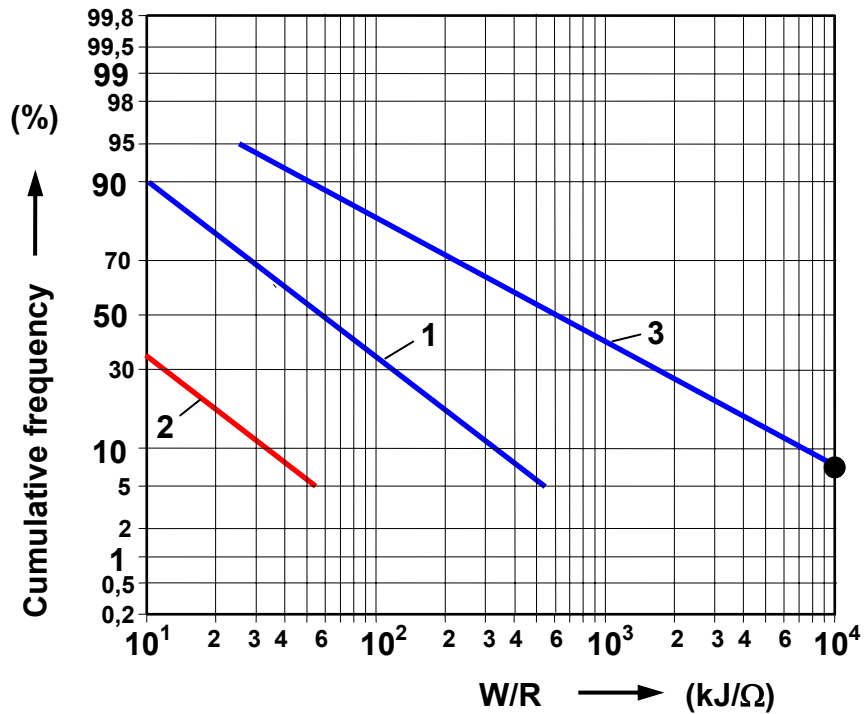


Fig. 12 - Cumulative frequency of the specific energy W/R according to CIGRE  
 1: Negative first stroke  
 2: Negative subsequent stroke  
 3: Positive stroke  
 • Fixed value in IEC 62305-1 for LPL 1

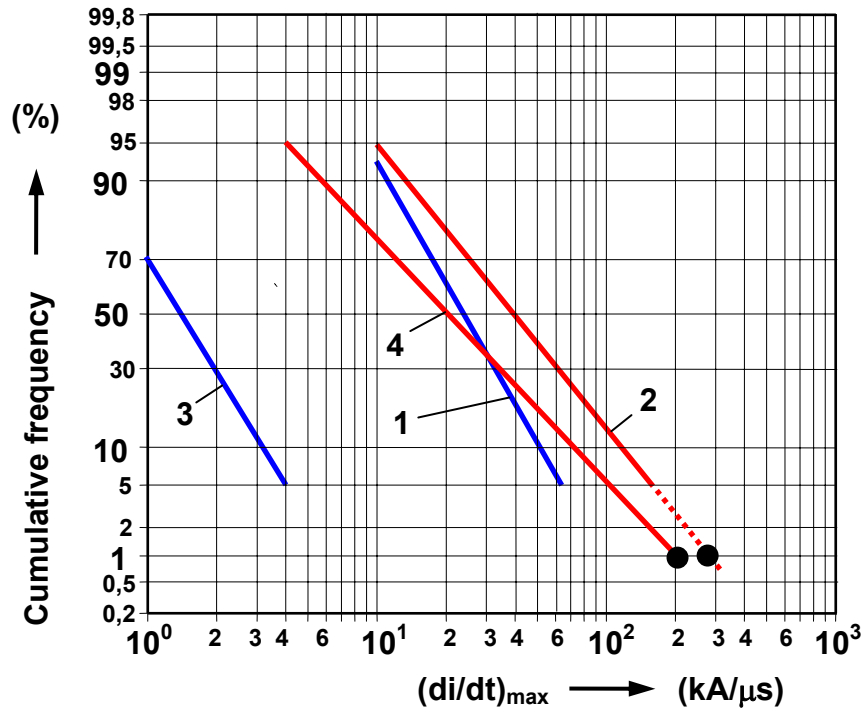


Fig. 13 – Cumulative frequency of the maximum current steepness  $(di/dt)_{max}$  according to CIGRE

- 1: Negative first stroke                      2: Negative subsequent stroke  
 3: Positive stroke                              4: Negative subsequent stroke:  $(di/dt)_{30-90\%}$

● Fixed value in IEC 62305-1 for LPL 1

#### H. Short stroke current for numerical analysis

Applying the commonly used double-exponential function, the short stroke current is given by the following formula:

$$i = \frac{i_{max}}{k} \cdot (e^{t/\tau_1} - e^{t/\tau_2}), \quad (5)$$

where  $i_{max}$  is the current maximum and  $k$  the correction factor of the current maximum. The coefficients  $\tau_1$  and  $\tau_2$  determine the decay time and the front time, respectively. With this function it is not possible to produce the short stroke currents according to the requirements of Table 4. For instance, the subsequent short stroke current of LPL I considered with the current peak of 50 kA and the rise time of  $T_1 = 0.25\mu s$  would have the maximum current steepness of about 545 kA/ $\mu s$  being about twice the fixed value. Furthermore, the current starts unrealistically with the maximum current steepness at the time instant  $t = 0$ , while the front of the first return stroke currents exhibits firstly a slowly rising portion followed by a fast current rise. These disadvantages can be avoided with the following formula:

$$i = \frac{i_{max}}{k} \cdot \frac{(t/\tau_1)^n}{1 + (t/\tau_1)^n} \cdot \exp(-t/\tau_2) \quad (6)$$

The current rise can be adjusted by the coefficients  $n$  and  $\tau_1$ . Finally, in IEC 62305-1 the following formula is fixed for the first and subsequent short stroke current:

$$i = \frac{i_{max}}{k} \cdot \frac{(t/\tau_1)^{10}}{1 + (t/\tau_1)^{10}} \cdot \exp(-t/\tau_2) \quad (7)$$

Table 5 contains the values of the coefficients for the different lightning protection levels LPL. Using these parameters, the current parameters are in concordance with the values fixed in Table 4. Fig. 14 and Fig. 15 depict the first and subsequent short stroke having the waveform 10/350  $\mu$ s and 0.25/100  $\mu$ s, respectively. It can be seen that the front of the short stroke currents starts with a slowly rising portion followed by a fast rising portion with the maximum current derivative approximately at the 50 % level of the peak current. The maximum current steepness is given by:

$$\left(\frac{di}{dt}\right)_{\max} \approx \sqrt{2} \frac{i_{\max}}{T_1} \quad (8)$$

From equation (2) the maximum current steepness follows to 280 kA/ $\mu$ s for the subsequent short stroke current of LPL I.

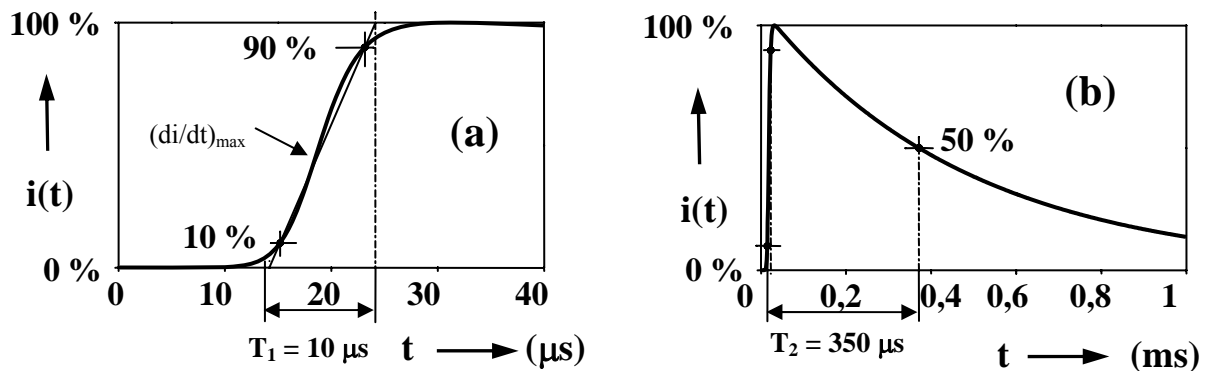


Fig. 14- Waveform of the first short stroke current (a) during the current rise and (b) during the current decay

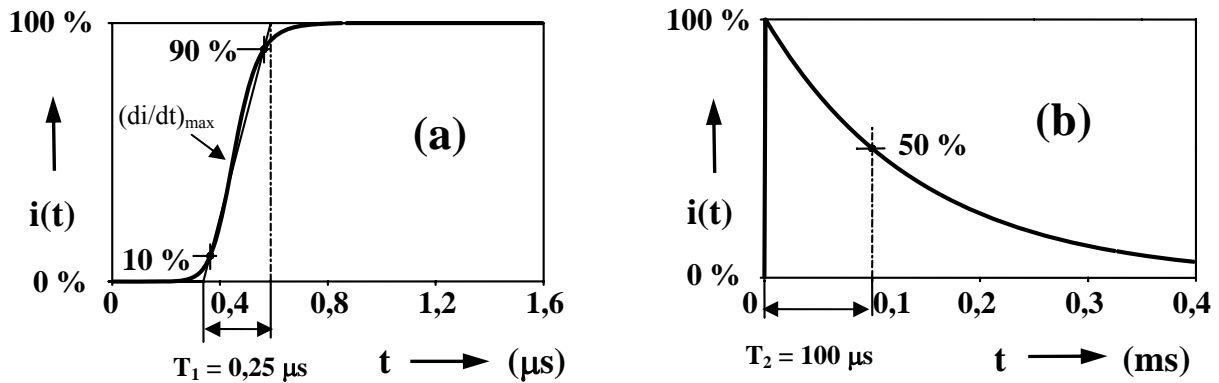


Fig. 15- Waveform of the subsequent short stroke current (a) during the current rise and (b) during the current decay

Table 5: Parameters for the current function according to IEC 62305-1

	First short stroke current			Subsequent stroke current		
	LPL			LPL		
	I	II	III-IV	I	II	III-IV
I(kA)	200	150	100	50	37.5	25
k	0.93	0.93	0.93	0.993	0.993	0.993
$\tau_1$ ( $\mu$ s)	19.0	19.0	19.0	0.454	0.454	0.454
$\tau_2$ ( $\mu$ s)	485	485	485	143	143	143

### I. Lightning current for testing

Deleterious effects, like heating and mechanical damage, are mainly related to first return strokes. The most important current parameters for testing are the current peak value  $i_{max}$ , the impulse charge  $Q_i$  and specific energy  $W/R$ . Therefore, the peak current  $I$ , the charge  $Q_{short}$  and the specific energy  $W/R$  are tested only for the first short stroke current, because these current parameters are much lower for the subsequent short stroke current. The front time  $T_1$  usually is of minor interest as it does not remarkably affect degrading or physical damage in most practical cases. Nevertheless  $T_1$  should be a typical value, not exceeding a few 10  $\mu s$ .

Due to the limitations of the test equipment, in laboratory test the fixed stroke currents can be realized only within certain tolerances. The test parameters and their tolerances are listed in Table 6. The waveform should be essentially unidirectional and the test parameters have to be obtained in the same test current.

For the long stroke current, the long stroke charge  $Q_{long}$  is fixed with the duration of 0,5s. The test parameters and the tolerances are listed in Table 7.

Table 6: Test parameters of the first short stroke

Test parameter	Unit	LPL			Tolerance
		I	II	III-IV	
Peak current I	kA	200	150	100	$\pm 10 \%$
Charge $Q_{short}$	C	100	75	50	$\pm 20 \%$
Specific energy $W/R$	MJ/ $\Omega$	10	5,6	2,5	$\pm 35 \%$

Table 7: Test parameters of the long stroke

Test parameter	Unit	LPL			Tolerance
		I	II	III-IV	
Charge $Q_{long}$	C	200	150	100	$\pm 20 \%$
Duration $T_{long}$	s	0,5	0,5	0,5	$\pm 10 \%$

The current steepness can be tested for the first short stroke and the subsequent short stroke. For these tests, there are no special requirements defined regarding the current decay. It is only necessary to meet the requirements of the current front shown in Fig. 16, where the current rise is fixed by the current value  $\Delta i$  and the time duration  $\Delta t$ . The associated test parameters are listed in Table 8.

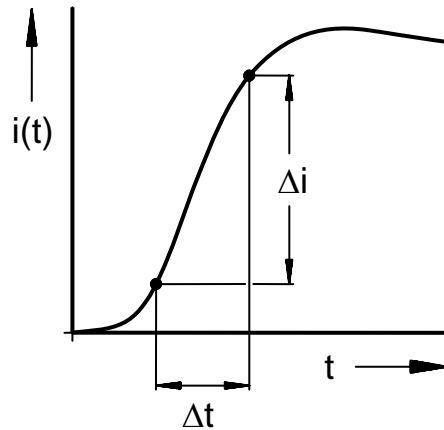


Fig. 16 - Definition of the current steepness for test purposes

Table 8: Test parameters to simulate the current steepness of the short strokes

Type of short stroke	Test parameter	Unit	LPL			Tolerance
			I	II	III-IV	
First	$\Delta i$	kA	200	150	100	$\pm 10 \%$
	$\Delta t$	$\mu s$	10	10	10	$\pm 20 \%$
Subsequent	$\Delta i$	kA	50	37,5	25	$\pm 10 \%$
	$\Delta t$	$\mu s$	0,25	0,25	0,25	$\pm 20 \%$

## 5 LABORATORY SIMULATING OF LIGHTNING CURRENTS

### A. Simulation of First Return Stroke Effects

High current impulse generators usually consist of a set of large high voltage capacitors  $C_{s/1} \dots C_{s/n}$  connected in parallel [40]. As an example, Fig. 17 shows the impulse current generator at the high voltage laboratory of the University of the Federal Armed Forces in Munich. The 24 individual surge capacitors  $C_{s/v}$  are arranged in form of a “U”. The object under test can be placed in the centre of the “U”.



Fig. 17- Example of an impulse current generator

The capacitor bank (Fig. 17 and Fig. 18) is slowly charged from a DC source to a high voltage  $U_{ch}$  (e.g. 100 kV) and then rapidly discharged via a starting switch  $S$  (usually a spark gap) over external wave forming elements  $R_{ext}$  and  $L_{ext}$  into the object under test with the load characteristics  $R_{load}$  and  $L_{load}$ . The connections inside the generator should be configured so as to minimize its internal resistance  $R_{int}$  and inductance  $L_{int}$ . Such a generator is characterized by its maximum charging voltage  $U_{ch}$  and the energy  $W$  stored in the capacitor bank  $C_s$

$$W = \frac{1}{2} \cdot C_s \cdot U_{ch}^2 \quad (9)$$

with  $C_s$  being the sum of all individual surge capacitors  $C_s = \sum_1^n C_{s/v}$ .

Essentially, the generator design shown in Fig. 18 forms an R-L-C circuit. Depending on the magnitude of the damping resistance  $R$ , three basic current waveforms may result from an R-L-C circuit (Fig. 19):

- $0 < R < 2 \sqrt{L/C_s}$  : under-critically damped (damped oscillating) current
- $R = 2 \sqrt{L/C_s}$  : critically damped (unidirectional) current
- $R > 2 \sqrt{L/C_s}$  : over-critically damped (unidirectional) current.

In order to obtain maximum current output, impulse current generators had to be operated in an under-critically damped mode. Under-critically damping, however, means that the current waveform is oscillatory, contrary to the unidirectional currents associated with natural lightning strokes.

To get a unidirectional waveform from an R-L-C circuit requires critical (or over-critical) damping. Critical damping is obtained by increasing the circuit resistance. This, however, means lower current peak values and wasting most of the energy, initially stored in the capacitor bank, by heating the generator's damping resistors. Critically damped R-L-C circuits, capable of generating peak currents of 100 kA ... 200 kA with a charge transfer of 50 C ... 100 C would become rather large and expensive. Therefore, they are used in practice only for generating impulse currents with a charge transfer of up to several tens of Coulombs.

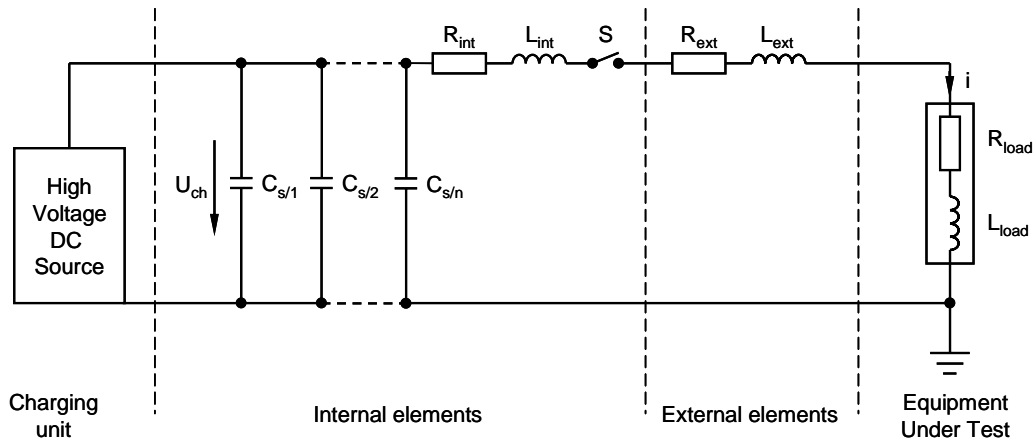


Fig. 18 - High current impulse generator

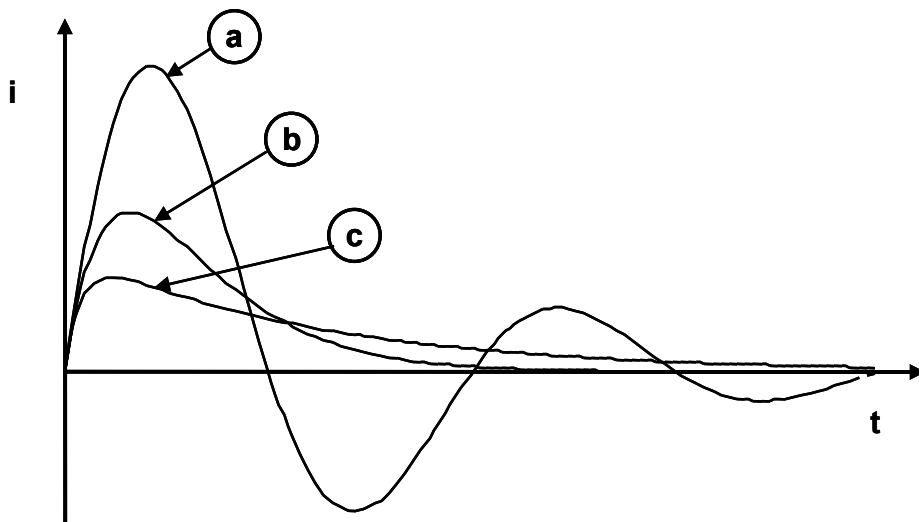


Fig. 19 - Basic current waveforms of an R-L-C circuit

- a: under-critically damped circuit
- b: critically damped circuit
- c: over-critically damped circuit



**B. Crowbar Technologies**

A very effective way to obtain a unidirectional current with a tolerable size of the capacitor bank is the use of a crowbar device in an R-L-C circuit [41 - 44]. The basic circuit diagram of such a generator is shown in Fig. 20.

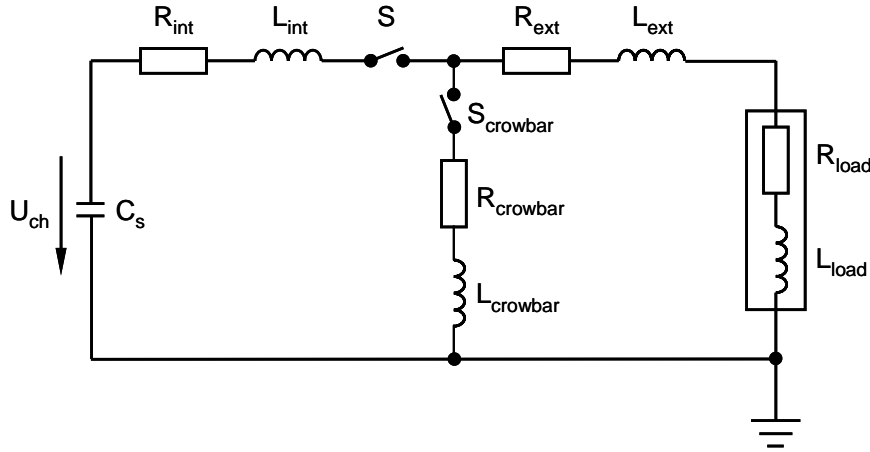


Fig. 20 - Circuit of an impulse current generator with crowbar device

The principle of operation of an impulse generator with crowbar device is illustrated in Fig. 21 [41, 42]. An external inductance  $L_{ext}$ , significantly larger than the internal inductance  $L_{int}$ , is inserted into the circuit. To obtain a high current peak value the generator is operated in a strong under-critically damped mode with low resistance. The discharge is initiated by a starting gap  $S$  at  $t = 0$ , while the crowbar device  $S_{crowbar}$  remains open. At the instant of the crest value of the current,  $t = T_{cr}$ , the crowbar device  $S_{crowbar}$  is closed. Most of the energy, initially stored in the capacitor bank, is at the instant  $T_{cr}$  transferred to the inductances  $L_{ext}$  and  $L_{load}$ . By shorting out the capacitors with the crowbar device the current is converted from an oscillatory to an exponentially decaying waveform.

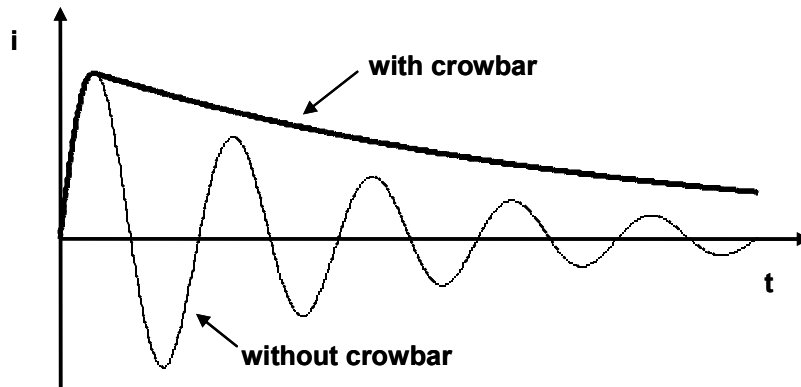


Fig. 21 - Principle of an impulse current generator with crowbar devices

The external resistance  $R_{ext}$  usually is composed of only the resistance of the copper bars used for connection and therefore can be quite low. The decay of the current, then, is proportional to the resistance of the object under test plus the resistance of the crowbar device. Thus, a major part (50 % and more) of the energy, originally stored in the capacitor bank, can be transferred into the object under test. Objects intended to handle high lightning currents inherently have to be of low resistance. Therefore, using crowbar technique, high impulse currents with decay times to half value of several 100  $\mu s$  can be obtained. An actual waveform is shown in Fig. 22.

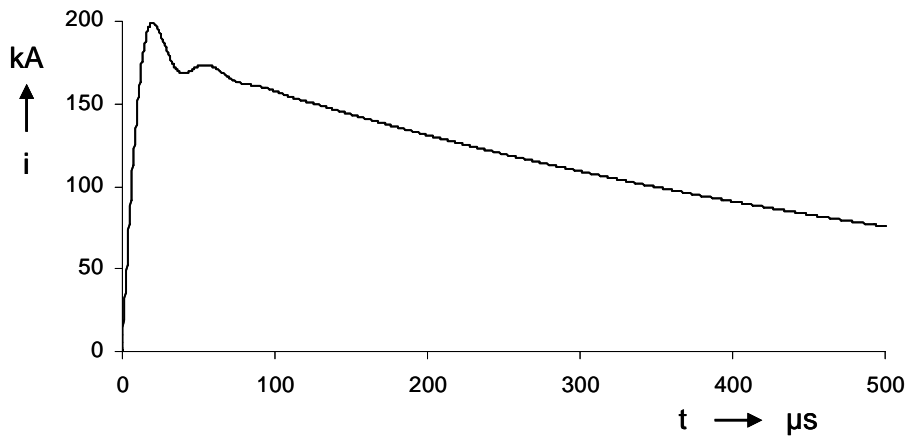


Fig. 22 - Actual waveform of an impulse current with crowbar device

### C. Simulation of subsequent return stroke effects

Magnetically induced over-voltages are mainly related to the high current steepness  $di/dt$  during the rise time portion of a stroke, while the induction during the slower decay is less important. The highest current steepness is found in negative subsequent strokes with values up to  $100 \text{ kA}/\mu\text{s}$  or  $200 \text{ kA}/\mu\text{s}$ . The maximum current steepness of a RLC-circuit is equal to the ratio of the charging voltage  $U_{ch}$  to the total inductance  $L$

$$di/dt_{\max} = \frac{U_{ch}}{L} \quad (15)$$

The generator design for simulating the high current steepness of negative subsequent strokes is much depended on the inductance of the object to be tested. Given a certain load inductance, attempts to simply increase the charging voltage yields little benefit. Increasing the charging voltage requires more insulation spacing, which in turn increases the generator circuit internal inductance. Therefore, specific measures to keep the internal inductance low or to boost the current front have to be applied. For such tests sophisticated and expensive generator equipment is necessary like low inductance Megavolt Marx-generators [45], lumped [46] or distributed [47] peaking circuits added to a current generators or exploding wires [48, 49].

### D. Generation of Long Duration Currents

Long duration currents are characterized by averaged currents of some 100 A lasting up to 500 ms and are resulting in a charge transfer  $Q_1$  of a few of 100 C. If a test standard does not require a rectangular waveform, long duration currents can be produced from a critically damped capacitor discharge. Rectangular waveforms are generated using a DC-source (Fig. 23) which is applied to the object under test via a resistor to adjust the required current amplitude.

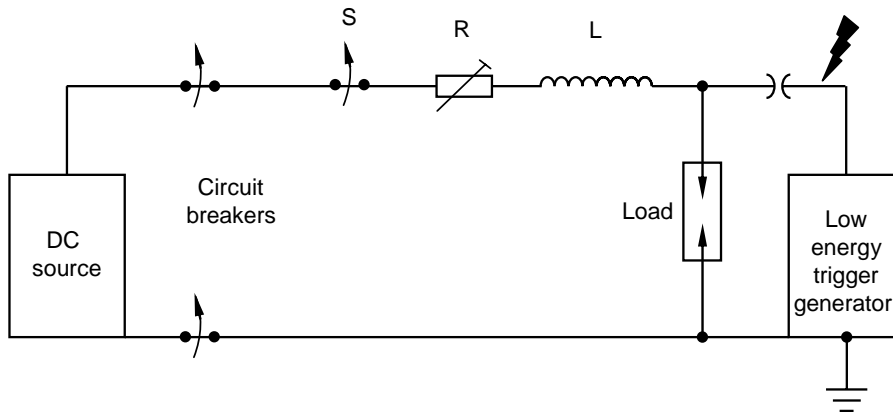


Fig. 23 - Long duration current generator

## 6 CURRENT PARAMETERS RELATED TO LIGHTNING INTERCEPTION

### A. Rolling sphere method

The rolling sphere method is suggested in IEC 62305 – 3 [50] to be used for the detection of possible striking points. This is a universal method and there are no limitations regarding the structure to be protected. Fig. 24 shows an example how to apply this method. A sphere with a certain radius  $r$  is rolled around and over the structure to be protected in all possible directions. Lightning strikes, then, are possible to any points touched by the sphere. The shaded areas are exposed to lightning interception and need a lightning protection. On the other hand, lightning strikes are excluded at all points not touched by the rolling sphere. The un-shaded areas are within the protected volume.

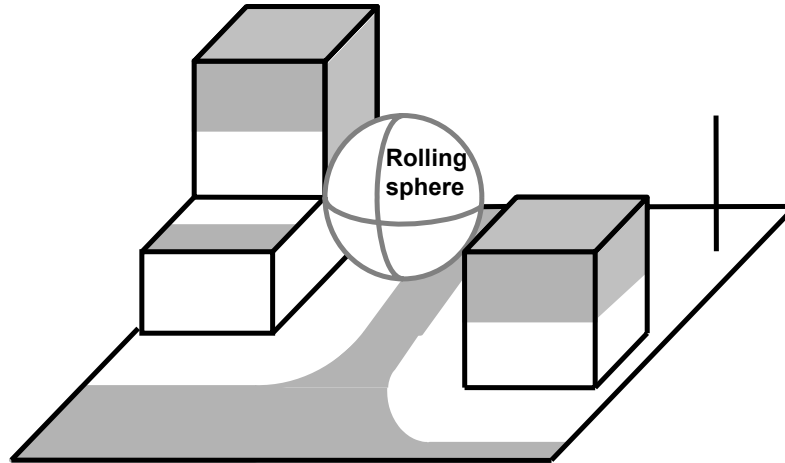


Fig. 24 - Application of the rolling sphere method to a structure to be protected.

### B. Fixing of the lightning current for the determination of possible striking points

Following the electro – geometric model the rolling sphere radius  $r$  is identical to the striking distance. The radius  $r$  (m) is correlated with the peak current  $i_{\max}$  (kA) of the first short stroke and it is given by the following relation [32]:

$$r = 10 \cdot i_{\max}^{0,65} \quad (16)$$

Table 9 contains the rolling sphere radii and the associated current peaks for the different LPL fixed in IEC 62305 – 1 [32]. The minimum values of the rolling sphere radius  $r$  define the interception efficiency of the lightning protection system LPS according to IEC 62305 – 3 [50]. Therefore, LPL I has the smallest rolling sphere radius, while LPL IV has the highest. The probability  $p$  denotes the percentage of lightning with a current peak lower than the current peak valid for the LPL. For these lightning, it cannot be excluded that they terminate inside the protected volume.

Fig. 25 shows again (see Fig. 10) the cumulative frequency of the current peak  $i_{\max}$  of the first negative stroke according to CIGRE. The positive return stroke is ignored, because the positive lightning contributes only by 10 % to the ground lightning.

For LPL I, the rolling sphere radius is fixed to  $r = 20$  m corresponding to the maximum current peak of 3 kA (see Table 9 and Fig. 25). It is accepted that 1 % of the lightning has smaller current peaks, while 99 % of the lightning has higher current peaks. This means that there is the residual risk that one percent of the lightning may terminate at the volume to be protected. For LPL IV the current maximum is increased to 16 kA resulting in the rolling sphere radius of 60 m. For LPL VI, direct lightning to the volume to be protected is excluded for the 84 % of lightning having higher current peaks, while the direct lightning strike cannot be excluded for the remaining rest of 16 % having lower current peaks than 16 kA.

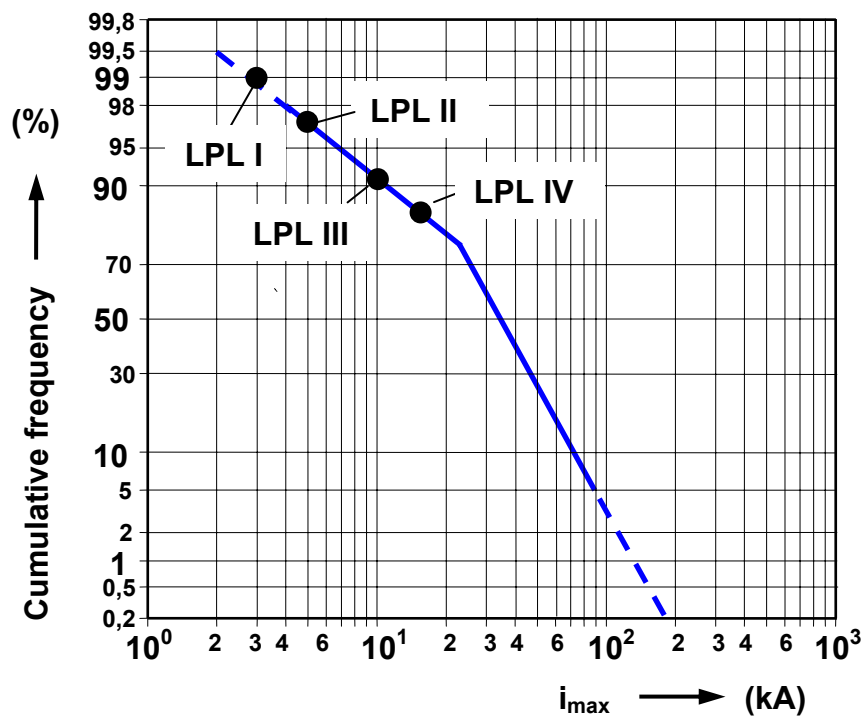


Fig. 25 - Cumulative frequency of the current peak  $i_{max}$  of the first negative stroke according to CIGRE

● Fixed values in IEC 62305-1 for LPL I-IV

Table 9: Fixed values in IEC 62305-1 to be used for the determination of possible striking points according to the different LPL. The fixed values comprise the rolling sphere radius  $r$ , of the associated current peak  $i_{max}$  and of the probability  $P$  of lightning having higher current peak than the fixed value.

LPL	I	II	III	IV
Current peak $i_{max}$	3 kA	5 kA	10 kA	16 kA
Rolling sphere radius $r$	20 m	30 m	45 m	60 m
Probability $p$	99 %	87 %	91 %	84 %

## 7 OUTLOOK

The lightning current parameters defined in the standard series IEC 62305 are mainly based on the direct measurements by *Berger* and co-workers in Switzerland. Meanwhile more recent direct current measurements were obtained from instrumented towers in Austria, Germany, Russia, Canada, and Brazil, as well as from rocket-triggered lightning. Further, modern lightning locating systems (LLS) report peak currents estimated from measured electromagnetic field peaks.

In spite of recent data on lightning current parameters, there are no new statistical distributions of current parameters. Therefore, CIGRE decided to set up a new working group to update its publications of 1975 [16] and 1980 [33]. Changes of lightning current parameters shall not be accepted in lightning protection standard until the results of the new CIGRE working group are available.

The scope is to address the new data with respect to engineering applications and to also include additional lightning parameters that are presently not on the CIGRE list or in the IEC standards (e.g. strokes per flash, interstroke interval, number of channels per flash, relative intensity of strokes within a flash, return-stroke speed etc.). Further on, more detailed information about less frequent, but potentially more destructive positive and bipolar lightning flashes is needed. Possible geographical, seasonal or other variations in lightning parameters will be accounted for.

## 8 REFERENCES

- [1] Grünewald, H., „Die Messung von Blitzstromstärken an Blitzableitern und Freileitungsmasten“, *Elektrotechnische Zeitschrift*, vol. 21, pp. 505-509, 1934.
- [2] Grünewald, H., „Die Messung von Blitzstromstärken an Blitzableitern und Freileitungsmasten“, *Elektrotechnische Zeitschrift*, vol. 22, pp. 536-539, 1934.
- [3] Zaduk, H., „Neuere Ergebnisse der Blitzstromstärkemessungen an Hochspannungsleitungen“, *Elektrotechnische Zeitschrift*, vol. 17, pp. 475 – 479, 1935.
- [4] Popolansky F., „Lightning current measurement on high objects in Czechoslovakia. Proc. of the 20th International Conference on Lightning Protection ICLP, Interlaken, report 1.3, 1990.
- [5] Kulikow, D., „Blitzströme“, Proc. of the 14th International Conference on Lightning Protection, Danzig, report R-1.05, 1978.
- [6] Miladowska, K., „Vergleichung der Blitzresultate von hohen Schornsteinen und den Zählern“, Proc. of the 14th International Lightning Conference ICLP, Danzig, Bericht R-1.04, 1978.
- [7] McEachron, K.B., „Lightning to the Empire State Building“, *Journal of the Franklin Institute*, vol. 227, no. 2, pp 149 – 217, 1939.
- [8] Garbagnati, E. and G.B. LoPiparo, „Lightning Parameters - Results of 10 years investigation in Italy“, International Aerospace Conference on Lightning and Static Electricity ICOLSE, Oxford, Report A1, 1982.
- [9] Geldenhuis, H., A. Eriksson and A. Bouon, „Fifteen years' data of lightning current measurement on a 60 m mast“, Proc. of the 19th International Conference on Lightning Protection ICLP, Graz, report R-1.7, 1988.
- [10] Schroeder, M., A. Soares, S. Visacro, L. Cherchiglia, and V. Souza, „Lightning current statistical analysis: Measurements of Morro do Cachimbo Station - Brasil“, Proc. of the 26<sup>th</sup> International Conference on Lightning Protection ICLP, Krakow, Poland, report 1a.4, 2002.
- [11] Brechow W.M. and W.P. Laronow, „Charakteristiken des Blitzes bei Einschlägen in hohe Objekte“, Proc. of the 16th International Conference on Lightning Protection ICLP, Budapest, report R-1.08, 1981.
- [12] Gorin, B.N., W.I. Lewitow and A.W. Schkiljew, „Einige Ergebnisse der Blitzstationenaufnahmen auf dem Ostankino-Fernsehturm“, Proc. of the 13th International Conference on Lightning Protection ICLP, Venice, report 1.9, 1976.
- [13] Gorin, B.N., W.I. Lewitow and A.W. Schkiljew, „Besonderheiten der Blitz einschläge in den Ostankino-Fernsehturm“, 13th International Conference on Lightning Protection ICLP, Venice, report 1.10, 1976.
- [14] Goto, Y., K. Narita, H. Komuro, and N. Honma, „Current waveform measurement of winter lightning struck an isolated tower“, 20th International Conference on Lightning Protection ICLP, Interlaken, report 1.9, 1990.
- [15] Miyake, K., T. Suzuki, K. Shinjou, „Characteristics of winter lightning currents on Japan sea coast“, *IEEE Transactions on Power Delivery*, vol. 7, no. 3, pp. 1450 – 1456, 1992.
- [16] Berger, K, R.B. Anderson and H. Kroeninger, „Parameters of lightning flashes“, *Electra*, vol. 41, pp. 23 – 37, 1975.
- [17] Berger, K., „Resultate der Blitzforschung auf dem Monte San Salvatore bei Lugano in den Jahren 1963 – 1971“, reprint of the authors.
- [18] Berger, K., E. Vogelsang, „Messungen und Resultate der Blitzforschung der Jahre 1955 ... 1963 auf dem Monte San Salvatore“, *Bulletin SEV*, vol. 56, no.1, pp. 2 – 22, 1965.
- [19] Berger, K., „Novel observations on lightning discharges: Results of research on Mount San Salvatore“, *Journal of the Franklin Institute*, vol. 283, no. 6, pp. 478 - 525, 1967.
- [20] Berger, K., „Methoden und Resultate der Blitzforschung auf dem Monte San Salvatore bei Lugano in den Jahren 1963 – 1971“, *Bulletin SEV*, vol. 87, no. 24, pp. 1403 – 1422, 1972.
- [21] Berger, K., „Blitzstrom-Parameter von Aufwärtsblitzen“, *Bulletin SEV*, vol. 69, no. 8, pp. 353 – 360, 1978.
- [22] Fuchs, F., E. U Landers, R. Schmid, R. and J. Wiesinger, „Lightning current and magnetic field parameters caused by lightning strikes to tall structures relating to interference of electronic systems“, *IEEE-Transactions on EMC*, vol. 40, no. 4, pp. 444 - 451, November 1998.
- [23] Diendorfer, G., M. Mair, W. Schulz, W. and W. Hadrian, „Lightning current measurements in Austria - Experimental setup and first results“, Proc. of the 25th International Conference on Lightning Protection ICLP, Rhodes, Greece, report 1.14, pp. 44 – 47, 2000.
- [24] Janischewskyi, W., A.M. Hussein, A.M., V. Shostak, I. Rusan, J.-X. Li, J.-S. Chang, „Statistics of lightning strikes to the Toronto Canadian National Tower (1978-1995)“ IEEE-Publication: SM 422-6 PWRD, 1996.
- [25] Montandon, E., and B. Beyerler, „The lightning measuring equipment on the Swiss PTT telecommunication tower at St. Chrischona, Switzerland“, Proc. of the 22nd International Conference on Lightning Protection (ICLP), Budapest, Hungary, report R 1c\_06, 1994.
- [26] Heidler, F., W. Zischank, and J. Wiesinger, „Statistics of lightning current parameters and related nearby magnetic fields measured at the Peissenberg tower“, Proc. of the 25th International Conference on Lightning Protection ICLP, Rhodes, Greece, report 1.19, pp. 78 – 83, 2000.
- [27] Newman, M.M., J.R. Stahmann, J.D. Robb, E.A. Lewis, S.G. Martin, S.V. Zinn, „Triggered lightning channel strokes at very close range“, *Journal of Geophysical Research*, vol. 72, no. 18, pp. 4761 – 4764, 1967.
- [28] Miyake, K., K. Horii, „Five years' experiences on artificially triggered lightning in Japan“, Proc. of the 7<sup>th</sup> IEE-Conference „Gas Discharges and their Application“, pp. 468 – 471, 1982.
- [29] Liu, X., C. Wang, Y. Zhang, Q. Xiao, D. Wang, Z. Zhou, C. Guo, „Experiment of artificially triggering lightning in China“, *Journal of Geophysical Research*, vol. 99, no. D5, pp. 10727 – 10731, 1994.
- [30] Depasse, P., „Statistics on artificially triggered lightning“, *Journal of Geophysical Research*, vol. 99, no. D9, pp. 186515 – 18522, 1994.
- [31] Uman, M.A., V. Rakov, K.J. Rambo, T.W. Vaught, M.I. Fernandez, D.J. Codier, R.M. Chandler, R. Bernstein and C. Golden, „Triggered-lightning experiments at Camp Blanding, Florida (1993-1995)“, *Transaction on IEE Japan*, vol. 117-B, no. 4, pp. 446 – 452, 1997.
- [32] IEC 62305-1, „Protection against lightning – Part 1: General principles“, IEC-standard, 2003.
- [33] Anderson, R.B.; Eriksson, A.J.: Lightning parameters for engineering application. *Electra* 69 (1980), S. 65 - 102.
- [34] Heidler, F., J. Wiesinger and W. Zischank, „Lightning currents measured at a telecommunication tower from 1992 to 1998“, 14th International Zurich Symposium on EMC, report 61J6, pp. 325 – 330, 2001.
- [35] Rakov, V., M.A. Uman and K.J. Rambo, „A review of ten years of triggered-lightning experiments in Camp Blanding, Florida“, *Journal of Atmospheric Research*, Vol. 76, pp. 503 – 517, 2005.
- [36] Fisher, R.J., G.H. Schnetzer, R. Thottappillil, V. Rakov, M.A. Uman and J.D. Goldberg, „Parameters of triggered lightning flashes in Florida and Alabama“, *Journal of Geophysical Research*, vol. 98, no. D12, pp. 22880-22902, December 1993.

- [37] Orville, R.E., and Silver, A.C.: Lightning ground flash density in the contiguous United States: 1992-95. *Monthly Weather Review*, 125, 1997, 631-638.
- [38] Orville, R.E., and Huffines, G.R.: "Lightning ground flash measurements over the contiguous United States: 1995-1997". *Monthly Weather Review* 127, 1999, 2693-2703.
- [39] Rakov, V.A., Uman, M.A.: "Lightning - Physics and effects", Cambridge University Press, 2003.
- [40] Hasse, P., Wiesinger, J., Zischank, W.: *Handbuch für Blitzschutz und Erdung. 5th Edition, Pflaum Verlag, München; 2006.*
- [41] Zischank, W.: *Simulation von Blitzströmen bei direkten Einschlägen.* etz, 105, 1984, pp. 12-17.
- [42] Zischank, W.: *A surge current generator with a double-crowbar sparkgap for the simulation of direct lightning stroke effects.* 5th International Symposium on High Voltage Engineering, ISH, Braunschweig 1987, paper 61.07.
- [43] Hourtane, J-L.: *DICOM: Current generator delivering the A, B, C, D waveform for direct lightning effects simulation on aircraft.* International Aerospace and Ground Conference on Lightning and Static Electricity ICOLSE, Bath 1989, paper 5A.5.
- [44] Landry, M.J., Brigham, W.P.: *UV laser triggering and crowbars used in the Sandia lightning simulator.* International Aerospace and Ground Conference on Lightning and Static Electricity, Orlando 1984, paper 46-1 - 46-13.
- [45] White, R.A.: *Lightning simulator circuit parameters and performance for severe threat, high-action-integral testing.* International Aerospace and Ground Conference on Lightning and Static Electricity, Orlando, 1984, paper 40-1.
- [46] Craven, J.D., Knauer, J.A., Moore, T.W., Shumpert, Th.H.: *A simulated lightning effects test facility for testing live and inert missiles and components.* International Aerospace and Ground Conference on Lightning and Static Electricity, Cocoa Beach 1991, paper 108\_1.
- [47] Perala, R.A., Rudolph, T.H., McKenna, P.M., Robb, J.D.: The use of a distributed peaking capacitor and a Marx generator for increasing current rise rates and the electric field for lightning simulation. International Aerospace and Ground Conference on Lightning and Static Electricity ICOLE, Orlando 1984, pp. 45-1 - 45-6.
- [48] Salge, J., Pauls, N., Neumann, K.-K.: *Drahtexplosionsexperimente in Kondensator-Entladekreisen mit großer Induktivität.* Zeitschrift für angewandte Physik, 29, 1970, pp. 339-343.
- [49] Zischank, W.: *Simulation of fast rate-of-rise lightning currents using exploding wires.* 21st International Conference on Lightning Protection, ICLP, Berlin 1992, paper 5.01.
- [50] IEC 62305-3, *Protection against lightning - Part 3: Physical damage to structures and life hazard*, IEC-standard, 2006